TITLE: Effects of Processing Parameters on the Laser Deposition
of High Temperature Superconducting Thin Films

AUTHOR(S): N. S. Nogar, R. Castain, R. C. Dye, S. Foltyn, R. E. Muenchausen,
and X. D. Wu

MASTER

Los Alamos

Los Alamos National Laboratory
Los Alamos, New Mexico 87545

DISTRIBUTION OF THIS DOCUMENT IS UNLIMITED

EFFECTS OF PROCESSING PARAMETERS ON THE LASER DEPOSITION OF HIGH TEMPERATURE SUPERCONDUCTING THIN FILMS

N. S. Nogar[a], R. Castain[a], R. C. Dye[a], S. Foltyn[a], R. E. Muenchausen[b] and X. D. Wu[b]

[a]Chemical and Laser Sciences Division, MS G738
[b]Exploratory Research and Development Center, MS K778
Los Alamos National Laboratory, Los Alamos, New Mexico 87545

ABSTRACT:
   Y_2O_3 pressed powders were ablated by pulses from a XeCl excimer laser, operating at 308 nm, 150 mJ/pulse, $\approx$15 nsec/pulse and 20 Hz. Emission spectra from Y^* and YO^* were recorded as a function of ambient oxygen pressure in the range 10^{-5} - 4×10^{-1} Torr, at a laser fluence of $\approx$ 4 J/cm^2. A kinetic model is developed to describe the results, and the application to production of laser-deposited high-temperature superconductor thin films is discussed.

INTRODUCTION:
   Laser ablation for the deposition of thin films is becoming a widely used technology. This process has some advantages relative to conventional deposition technologies [1,2] including rapid growth rates, the ability to congruently evaporate multicomponent targets, and the production of high-energy (eV) atoms, molecules, ions and clusters which enhance the production of epitaxial films. Laser ablation has been used most recently for the production of high-temperature superconducting (HTSC) thin films [3-5].

   Recent work in this laboratory has demonstrated the production of high-quality epitaxial HTSC thin films using the laser deposition technique [6-8]. In this process, a pressed oxide target, containing a stoichiometric mixture of yttrium, barium and copper is ablated at fluences $\approx$4 J/cm^2. The vaporized material passes through a low-pressure oxygen atmosphere, 0.2 Torr, and is subsequently deposited on a heated (700 °C) substrate. The film is cooled in a relatively high-pressure oxygen atmosphere, 200 Torr.

   Despite efforts to understand the chemistry of this process [9], little is known about the gas phase or surface chemistry occuring during the deposition process. In an effort to elucidate the mechanisms for the gas phase chemistry, we have undertaken a study of single-component metal and metal oxide laser ablation. In this work, we report on the ablation of Y_2O_3, with a XeCl excimer laser.

EXPERIMENTAL:
   The bulk of the apparatus has been described previously [6] . Briefly, the deposition chamber consists of a modified six way 6" dia. stainless steel cross, as shown in Figure 1. Load locks are provided for target and substrate introduction to minimize pumping times. The target can be rotated in conjunction with horizontal

rastering of the laser beam while the substrate is rotated to ensure uniform thickness (±10%) across the substrate diameter. Provisions are made to heat the substrate, either indirectly on a Ni block or radiatively. Processing gases can be introduced into the deposition chamber using mass flow control to maintain a constant pressure or by a pulsed valve. The excimer laser used in these experiments produced 200 mJ, 20 nsec pulses at 308 nm and a repetition rate of 20 Hz.
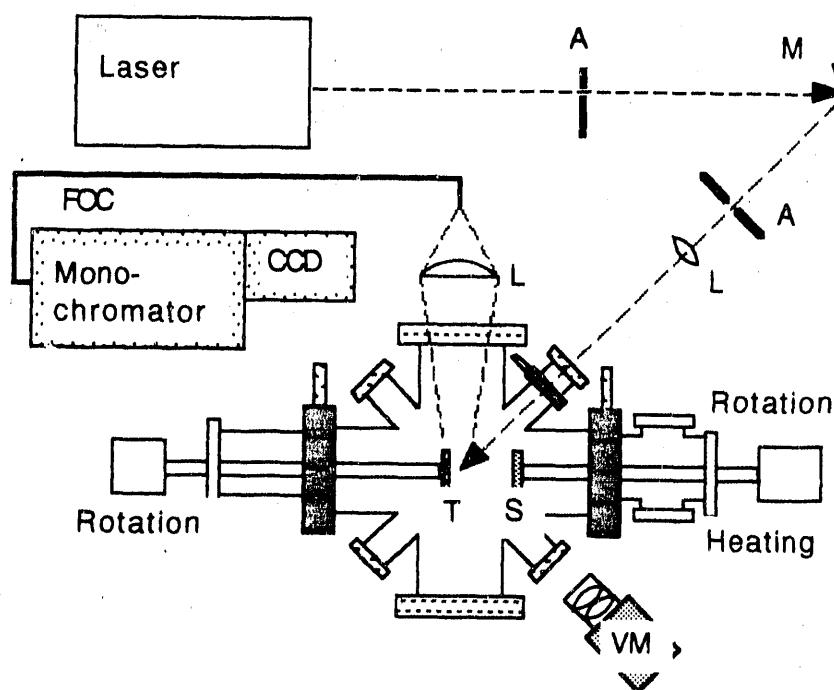

Figure 1. Schematic of the experimetnal apparatus. Symbols: A, aperture; M, mirror; L, lens; FOC, fiber optic cable; CCD, charge-coupled device; T, target; S, substrate; VM, video monitor.

Additionally, for the experiments described here, the plume optical emission was collected and analyzed. Light was collected by a 7.5 cm. diameter, 500 cm focal length quartz lens, and focussed onto either a photodiode or the end of a (200 μm diameter) multi-mode fiber optic cable (FOC), 10 m in length. The photodiode was used for total intensity measurements. The distal end of the fiber optic cable was coupled to an 0.5 m monochromator equipped with a gated, intensified CCD camera for spectrally resolved detection.

RESULTS AND DISCUSSION:
In previous experiments [9] , the plume resulting from ablation of a stoichiometric Y-Ba-Cu-O target was sampled mass spectrometrically . In these experiments, gas-phase Cu, Cu_2, Ba, and Y were detected, along with minor amounts of BaO, and their velocity distributions characterized. It is interesting that in this experiment, where the solid material was ablated into a vacuum, few oxide species were detected, suggesting that the oxygen incorporated into the HTSC thin films during the laser deposition process originates in the processing atmosphere, rather than in the solid

target material. In order to explore this hypothesis further, we have obtained data on chemical speciation under processing conditions: that is, oxygen pressures from 0.001 to 0.4 torr.

Emission spectra were obtained from the plume in the spectral region near 600 nm, where both atomic yttrium emission (Y^*) and yttrium monoxide emission (YO^*) could be observed. Figure 2 displays a spectrum obtained at an oxygen pressure of 2×10^{-1} torr. The detector was gated to integrate signal for the duration of the emission pulse, ≈ 10 µsec. The two starred transitions in Fig. 2 correspond to Y^*, while most of the remaining features are due to YO^*. The Y^* emissions are from the $^2D_{1/2}$ and $^2D_{3/2}$ states to the $^2D_{3/2}$ ground electronic state, while the YO^* emission is from the A $^2\Pi_{3/2,1/2}$ levels to the $^2\Sigma^+$ ground state [11,12]. All YO^* features are due to $v' = v''$ transitions, with the 0-0 transition being the most intense, 1-1 less intense, etc.
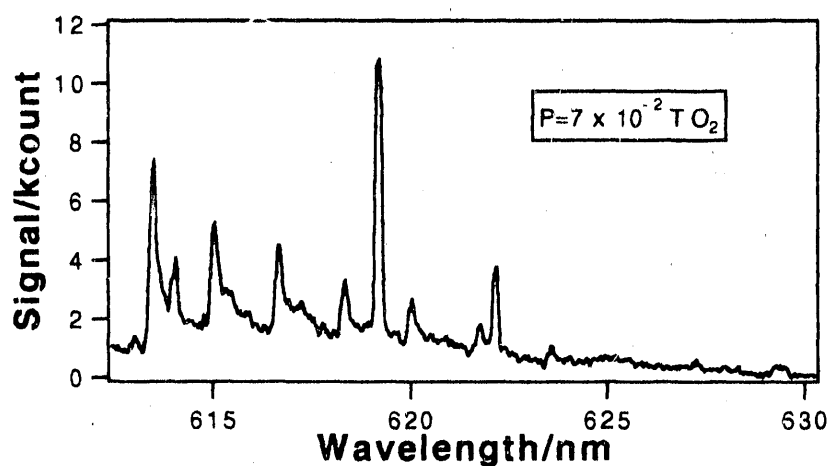

Figure 2. Emssion spectrum from interaction of material ablated from Y_2O_3 target with 7×10^{-2} torr of O_2.
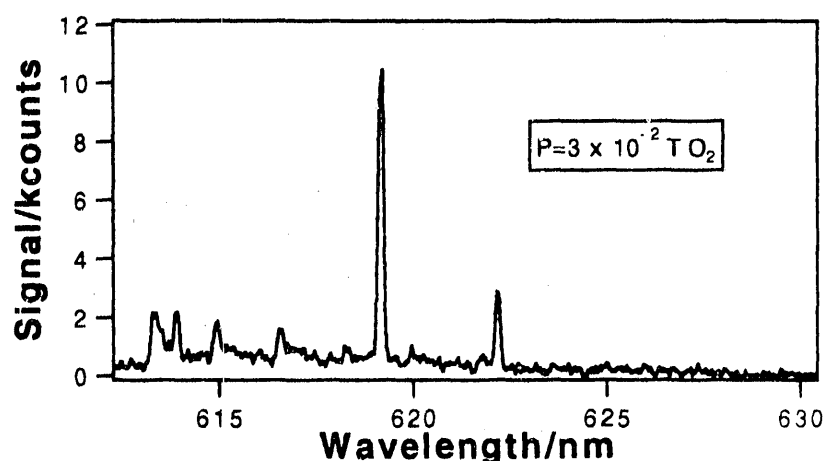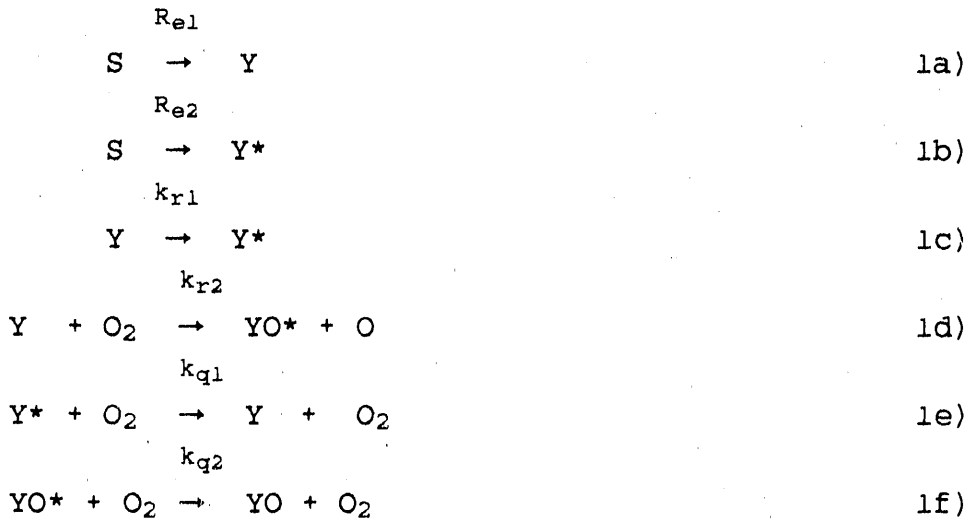

Figure 3. Emssion spectrum from interaction of material ablated from Y_2O_3 target with 3×10^{-2} torr of O_2.

The ratio of YO* to Y* emission was found to change dramatically with pressure of the ambient oxygen atmosphere. Figure 3 shows a spectrum similar to Fig 2, but obtained at an oxygen pressure of 3×10^{-2} torr. It can be seen that the emission due to YO* is dramatically reduced, relative to the spectrum in Fig. 2. In general, it was observed that the ratio YO*/Y* increased linearly with pressure at low oxygen pressures, and approached a limiting value at pressures ≥ 0.4 torr. No YO* emission was observed at oxygen pressures less than 10^{-3} torr, indicating that YO* is not formed directly from the solid material.

In order to interpret these results, a kinetic model was developed, based on the following sequence of six reactions:

$$S \xrightarrow{R_{e1}} Y \qquad\qquad\qquad 1a)$$

$$S \xrightarrow{R_{e2}} Y* \qquad\qquad\qquad 1b)$$

$$Y \xrightarrow{k_{r1}} Y* \qquad\qquad\qquad 1c)$$

$$Y + O_2 \xrightarrow{k_{r2}} YO* + O \qquad\qquad 1d)$$

$$Y* + O_2 \xrightarrow{k_{q1}} Y + O_2 \qquad\qquad 1e)$$

$$YO* + O_2 \xrightarrow{k_{q2}} YO + O_2 \qquad\qquad 1f)$$

Here, S indicates the solid target, Y and YO are gas-phase atoms and molecules, the symbol "*" indicates electronic excitation, and the R's and k's are rates and rate constants, respectively, for the indicated processes. Applying the steady-state approximation to this set of reactions results in a set of three coupled differential equations relating Y, Y*, and YO*. These equations can be solved for the ratio of emission intensities. The result is shown in simplified form below:

$$\frac{[YO^*]}{[Y^*]} = \frac{A [O_2]}{B + C [O_2]} \qquad\qquad 2)$$

where the constants A,B, and C are sums of products of the rates and rate constants, and $[O_2]$ represents the oxygen pressure. This result clearly obeys the correct limiting forms. At zero pressure, $[YO^*]/[Y^*] \rightarrow 0$, at low pressure $[YO^*]/[Y^*] \propto (A/B)[O_2]$, and at high pressure, $[YO^*]/[Y^*] \propto (A/C) =$ constant.

In addition, we have demonstrated [10] an excellent fit of equation 2) to the experimental data over the entire experimental pressure range (10^{-3} - 0.4 torr), for a

In addition, we have demonstrated [10] an excellent fit of equation 2) to the experimental data over the entire experimental pressure range (10^{-3} - 0.4 torr), for a temperature $\approx$2000K (see below). In this calculation, we assumed formation rates constants $R_{\theta 1} = R_{\theta 2} \approx 1 \times 10^{20}$ molec/cm³-sec, resulting from the ablation of 10 ng of material during a 100 nsec surface thermal transient, into a volume of $\approx$10 cm³. Rate constants k_{r2} and k_{q2} are known from the literature [12,13] to be 2×10^{-9} cm³/molec-sec. The unknown constants k_{r1} and k_{q1} were allowed to vary to produce the best fit to the experimental data; best-fit values were $k_{r1} = 3 \times 10^7$ sec⁻¹ (this reaction is assumed to be pseudo-first-order, with the transition effected primarily by electrons present in the laser generated plasma) and $k_{q1} = 3 \times 10^{-9}$ cm³/molec-sec.
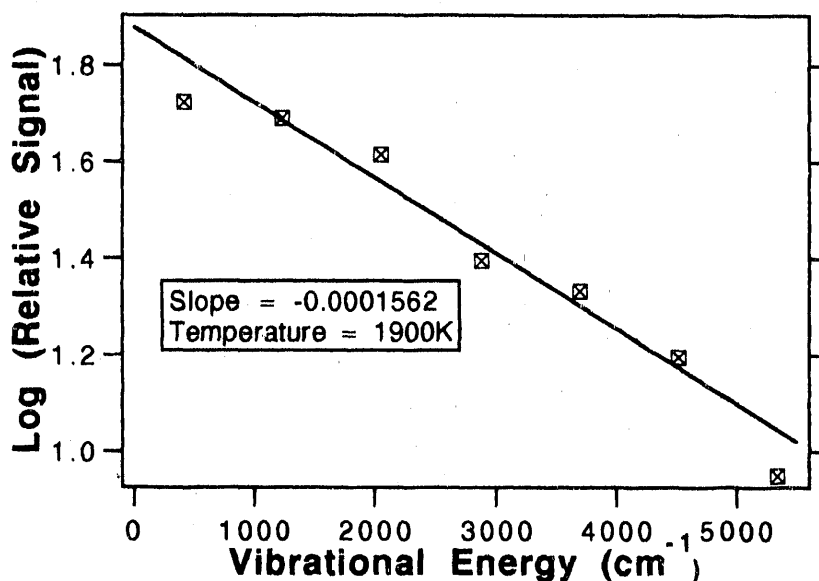

Figure 4. Determination of the vibrational temperature. The slope of this plot yields an effective temperature for the vibrational manifold.

In order to further characterize the plume chemistry and dynamics, the YO* vibrational temperature was obtained from the vibrational progression seen in Fig 2). The results are shown in Fig. 4), where the Log(intensity) for each vibrational transition is plotted against the energy for that particular vibrational level. The intensity of each transition is assumed proportional to the peak height, and peak heights are not corrected for line strength, since the Franck-Condon factors for all $v' = v''$ transitions in YO* are near unity. The slope of this plot yields an effective temperature for the vibrational manifold of $\approx$2000K.

CONCLUSIONS

These results, together with out earlier observations, confirm that the principal source for oxygen incorporated into laser-deposited HTSC thin films is the processing atmosphere, rather than oxygen in the target material. This has been confirmed both by mass spectrometry, and by the current experiments in emission spectroscopy.

Clearly, the absence of any YO* at low oxygen pressures indicates that direct production of YO* from the solid is a low-probability process, while the observation of Y* at these same pressures suggests that it is formed directly in the ablation event, or in the plasma formed directly above the surface. The reaction of ground state yttrium atoms with molecular oxygen is shown to be the dominant mechanism for production of YO*. Quenching of the emission by molecular oxygen is shown to be significant at pressures above $\approx 10^{-1}$ torr.

REFERENCES

1. J. T. Cheung and H. Sankur. *CRC Crit. Rev. Sol. St. Mat. Sci.* , 15, 63-109 (1988).
2. H. Sankur and J. T. Cheung. *Appl. Phys. A* , **A47**, 271-284 (1988).
3. T. Venkatesan, Xindi Wu, Arun Inam, Chuan C. Chang, Manjanain S. Hegde and Barundeb Dutta. *Ieee J. Quantum Electron.*, 25, 2388-93 (1989).
4. J. Narayan, N. Biunno, R. Singh, O. W. Holland and O. Auciello. *Appl. Phys. Lett.*, 51, 1845-7 (1987).
5. C. C. Chang, X. D. Wu, A. Inam, D. M. Hwang, T. Venkatesan, P. Barboux and J. M. Tarascon. *Appl. Phys. Lett.* , 53, 517-19 (1988).
6. R. E. Muenchausen, K. M. Hubbard, S. Foltyn, C. Jenkins, R. C. Estler and N. S. Nogar. *Appl. Phys. Lett.* , 56, 578 (1990).
7. X. D. Wu, *et al. Appl. Phys. Lett.* , **56**, 1481-3 (1990).
8. X. D. Wu, *et al. Appl. Phys. Lett.* , **57**, 523-525 (1990).
9. R. C. Estler and N. S. Nogar. *J. Appl. Phys.* , in press, (1990).
10. R. C. Dye, R. E. Muenchausen and N. S. Nogar. *Chem. Phys. Lett.* , submitted, (1991).
11. D. M. Manos and J. M. Parson, *J. Chem. Phys*, **63**, 3575 (1975); *ibid*, **69**, 231 (1978).
12. C. L. Chalek and J. L. Gole, *Chem. Phys.* 19, 59 (1977); ibid, *J. Chem. Phys.* , 65, 2845 (1976).
13. T. Wijchers, H. A. Dijkerman, P. J. Th. Zeegers and C. Th. J. Alkemade, *Chem. Phys.* 91, 141 (1984).

END

DATE FILMED

01 / 23 / 91